OPEN ACCESS
IOP Publishing
Journal of Physics A: Mathematical and Theoretical
J. Phys. A: Math. Theor. **55** (2022) 505005 (20pp)
https://doi.org/10.1088/1751-8121/acb097

Analytical results for the entanglement dynamics of disjoint blocks in the XY spin chain

Gilles Parez[1,*] and Riccarda Bonsignori[2]

[1] Centre de Recherches Mathématiques (CRM), Université de Montréal, PO Box 6128, Centre-ville Station, Montréal, Québec H3C 3J7, Canada
[2] Ruđer Bošković Institute, Bijenička cesta 54, 10000 Zagreb, Croatia

E-mail: gilles.parez@umontreal.ca

Received 24 October 2022; revised 6 December 2022
Accepted for publication 5 January 2023
Published 19 January 2023

Abstract
The study of the dynamics of entanglement measures after a quench has become a very active area of research in the last two decades, motivated by the development of experimental techniques. However, exact results in this context are available in only very few cases. In this work, we present the proof of the quasiparticle picture for the dynamics of entanglement entropies for two disjoint blocks in the XY chain after a quantum quench. As a byproduct, we also prove the quasiparticle conjecture for the mutual information in that model. Our calculations generalize those presented in Fagotti and Calabrese (2008 *Phys. Rev.* A 78 010306) to the case where the correlation matrix is a block-Toeplitz matrix, and rely on the multidimensional stationary phase approximation in the scaling limit. We also test the quasiparticle predictions against exact numerical calculations, and find excellent agreement. In the case of three blocks, we show that the tripartite information vanishes when at least two blocks are adjacent.

Keywords: entanglement dynamics, disjoint intervals, XY spin chain

(Some figures may appear in colour only in the online journal)

* Author to whom any correspondence should be addressed.

Original Content from this work may be used under the terms of the Creative Commons Attribution 4.0 licence. Any further distribution of this work must maintain attribution to the author(s) and the title of the work, journal citation and DOI.

1. Introduction

Understanding the nonequilibrium dynamics of quantum many-body systems is a question that has been at the heart of quantum mechanics since its early days [1]. For the last twenty years, this field of research has experienced a renewed interest, due to groundbreaking cold-atom and ion-trap experiments that managed to simulate the unitary evolution of closed systems on long time scales [2–6], as well as an intense theoretical activity [7]. A key aspect is that quantum entanglement and its dynamics out of equilibrium play a large role in our understanding of fundamental problems, such as the equilibration and thermalisation of isolated many-body systems [7–12] and the emergence of thermodynamics [13–16]. Moreover, several experiments managed to measure entanglement-related quantities [17–23].

The simplest protocol to drive a quantum system out of equilibrium is known as a *quantum quench* [24, 25]. Consider a system described by a Hamiltonian $H(\lambda)$, where λ is a set of external parameters. In the quench protocol, the system is prepared in the groundstate of some initial Hamiltonian $H(\lambda_0)$, and at time $t=0$ the parameters are quenched from λ_0 to λ_1 such that $[H(\lambda_0),H(\lambda_1)]\neq 0$. For $t>0$, the system evolves unitarily under the action of the post-quenched Hamiltonian $H(\lambda_1)$. Because the two Hamiltonians do not commute, the subsequent dynamics is non-trivial. In particular, the investigation of entanglement dynamics after a quantum quench received considerable attention over the last two decades [26–29].

For a quantum many-body system in a pure state $|\psi\rangle$, one is typically interested in the entanglement between a subsystem A and its complement, traditionally denoted B. The so-called *Rényi entropies* are defined from the reduced density matrix $\rho_A = \mathrm{Tr}_B(|\psi\rangle\langle\psi|)$ as

$$S_n^A = \frac{1}{1-n}\log \mathrm{Tr}\rho_A^n. \tag{1}$$

The limit $n\to 1$ of the Rényi entropies yields the celebrated *entanglement entropy* [30]. It is the von Neumann entropy of the reduced density matrix of subsystem A, namely

$$S_1^A \equiv \lim_{n\to 1} S_n^A = -\mathrm{Tr}(\rho_A \log \rho_A). \tag{2}$$

Rényi entropies quantify the entanglement between A and B, irrespective of the geometry of A. In many cases considered in the literature, A is a connected spatial region, such as a segment in a one-dimensional chain. However, the case where A consists of disjoints blocks has also generated interest [31–36]. Let us consider the situation where $A = A_1 \cup A_2$ consists of two blocks A_1 and A_2. From the entanglement entropies of the two blocks $S_n^{A_1\cup A_2}$, one defines the mutual information as

$$I_1^{A_1:A_2} = S_1^{A_1} + S_1^{A_2} - S_1^{A_1\cup A_2}, \tag{3}$$

as well as the Rényi mutual information

$$I_n^{A_1:A_2} = S_n^{A_1} + S_n^{A_2} - S_n^{A_1\cup A_2}. \tag{4}$$

Here, S_n^X, $X = A_1, A_2, A_1\cup A_2$, is the Rényi entropy from equation (1) where the reduced density matrix is obtained by tracing out the degrees of freedom of the complement of X from the total pure-state density matrix $\rho = |\psi\rangle\langle\psi|$. The mutual information is not *per se* an entanglement measure between A_1 and A_2 because it also contains classical correlations [37, 38], and a proper measure of entanglement in that context is instead the entanglement negativity [39]. However, both the mutual information and the negativity share important properties, both in [40] and out of equilibrium [41–43], and we relegate the study of the negativity to forthcoming investigations.

For a tripartite system $A = A_1 \cup A_2 \cup A_3$, a relevant quantity that characterizes multipartite entanglement is the tripartite information $I_n^{A_1:A_2:A_3}$. It is defined as [44]

$$I_n^{A_1:A_2:A_3} = I_n^{A_1:A_2} + I_n^{A_1:A_3} - I_n^{A_1:(A_2\cup A_3)} \tag{5}$$

and measures the extensiveness of the mutual information. In particular, a negative tripartite information indicates multipartite entanglement, and it is related to quantum chaos and scrambling [45–47]. In the context of two-dimensional systems where A_1, A_2, A_3 are adjacent regions, the tripartite information coincides with the celebrated topological entanglement entropy [48]. Very recently, the tripartite information was investigated in the context monitored spin chains [49] and quantum quenches [50]. While it vanishes at all times for many quench protocols, the authors of [50] show that in some cases its dynamics yields universal information about the system.

In integrable models, the quasiparticle picture [27–29, 51, 52] describes the growth of entanglement in time after a global quench, in terms of ballistic propagation of pairs of quasiparticles of opposite momentum, that spread entanglement and correlations through the system. In the case of disjoint subsystems, the quasiparticle picture can be adapted to describe the dynamics of the mutual information [41] and the entanglement negativity [53]. The quasiparticle picture also describes the growth of symmetry-resolved entanglement [54–56], and it has recently been generalized to the case of dissipative free fermionic and bosonic systems [57–61].

While the quasiparticle picture provides impressive quantitative results that have been checked extensively through numerical investigations, *ab initio* and analytical results for the entanglement dynamics after a quench remain scarce in the literature. In a seminal paper, Fagotti and Calabrese computed the complete time dependence of the entanglement entropy of a single interval after a quench in the XY chain [26]. Their derivation used the Toeplitz-matrix representation of the correlation matrix and multidimensional phase methods. However, a similar derivation for the case of disjoint blocks is still lacking. We also mention recent exact results for the negativity dynamics in dissipative models [60, 61] and quantum circuits [43]

In this paper, we provide the analytical derivation of the quasiparticle picture for the entanglement entropies of two disjoint blocks in the XY chain in presence of transverse field, generalizing the results of [26]. As a byproduct, this allows us to prove the quasiparticle picture result for the mutual information. Moreover, we show that the tripartite information vanishes at all times for the quench protocol we consider, and argue more generally that the quasiparticle picture implies a vanishing tripartite information. Finally, we mention that these calculations for the entropy dynamics of disjoint blocks have already been advertised and used in the context of symmetry-resolved entanglement measures [55, 56].

This paper is organized as follows. In section 2 we introduce the XY model and express the related entanglement measures in terms of the two-point correlation matrix after a quench. We discuss the quasiparticle conjecture for the entanglement dynamics in section 3, and give the analytical proof for the case of two disjoint blocks in section 4. We conclude in section 5 with a summary of the results and byproducts of our proof, and discuss further research directions.

2. The XY spin chain and entanglement dynamics

In this section we review the XY spin chain and its diagonalization. We also specify the quench protocol under consideration and recall the definition of the Rényi entropies and mutual information in terms of the two-point correlation matrix. Finally, we review the quasiparticle picture for the entanglement dynamics, both in the case where the subsystem consists of one or multiple blocks of contiguous sites.

2.1. The quenched XY spin chain

We consider the spin-$1/2$ XY spin chain in a transverse magnetic field with periodic boundary conditions. The Hamiltonian is

$$H(\gamma,h)=-\sum_{j=1}^{L}\left(\frac{1+\gamma}{4}\sigma_j^x\sigma_{j+1}^x+\frac{1-\gamma}{4}\sigma_j^y\sigma_{j+1}^y+\frac{h}{2}\sigma_j^z\right), \tag{6}$$

where γ is the anisotropy parameter, h is the external magnetic field, L is the size of the system and σ_j^α are the Pauli matrices at site j. The model can be solved via the Jordan–Wigner transformation, which maps the system into a free Fermi gas in the presence of an external potential [62].

We consider the following quench protocol. At time $t=0$, the system is prepared in the groundstate $|\psi_0\rangle$ of the Hamiltonian $H(\gamma_0,h_0)$ with some initial anisotropy and magnetic field γ_0 and h_0. The parameters are then quenched to the values γ and h, and for $t>0$ the time-evolved state is

$$|\psi(t)\rangle=\mathrm{e}^{-\mathrm{i}tH(\gamma,h)}|\psi_0\rangle. \tag{7}$$

In order to study the time evolution of the entanglement measures, it is useful to introduce the Majorana operators

$$a_{2j-1}=\left(\prod_{k=1}^{j-1}\sigma_k^z\right)\sigma_j^x, \qquad a_{2j}=\left(\prod_{k=1}^{j-1}\sigma_k^z\right)\sigma_j^y, \tag{8}$$

that satisfy

$$a_{2j-1}=c_j+c_j^\dagger, \quad a_{2j}=\mathrm{i}(c_j-c_j^\dagger), \quad \{a_m,a_n\}=2\delta_{m,n}, \tag{9}$$

where $c_j,c_j^\dagger$ are the canonical spinless fermionic operators. For a subsystem A consisting of ℓ contiguous spins, the time-dependent correlation matrix $\Gamma_A(t)$ is a $2\ell\times 2\ell$ matrix built from 2×2 blocks [52] as

$$\langle\psi(t)|\begin{pmatrix}a_{2m-1}\\ a_{2m}\end{pmatrix}\cdot\begin{pmatrix}a_{2n-1} & a_{2n}\end{pmatrix}|\psi(t)\rangle=\delta_{m,n}+\mathrm{i}[\Gamma_A(t)]_{m,n}, \qquad 1\leqslant m,n\leqslant\ell. \tag{10}$$

More explicitly, the correlation matrix is a block-Toeplitz matrix

$$\Gamma_A(t)=\begin{pmatrix}\Pi_0 & \Pi_1 & \cdots & \Pi_{\ell-1}\\ \Pi_{-1} & \Pi_0 & & \vdots\\ \vdots & & \ddots & \vdots\\ \Pi_{1-\ell} & \cdots & \cdots & \Pi_0\end{pmatrix}, \qquad \Pi_j=\begin{pmatrix}-f_j & g_j\\ -g_{-j} & f_j\end{pmatrix}. \tag{11}$$

In the large-L limit, f_j and g_j read [26]

$$\begin{aligned}f_j&=\mathrm{i}\int_{-\pi}^{\pi}\frac{\mathrm{d}k}{2\pi}\mathrm{e}^{-\mathrm{i}kj}\sin\Delta_k\sin(2\epsilon_k t),\\ g_j&=\int_{-\pi}^{\pi}\frac{\mathrm{d}k}{2\pi}\mathrm{e}^{-\mathrm{i}kj}\mathrm{e}^{-\mathrm{i}\theta_k}\left(\cos\Delta_k+\mathrm{i}\sin\Delta_k\cos(2\epsilon_k t)\right),\end{aligned} \tag{12}$$

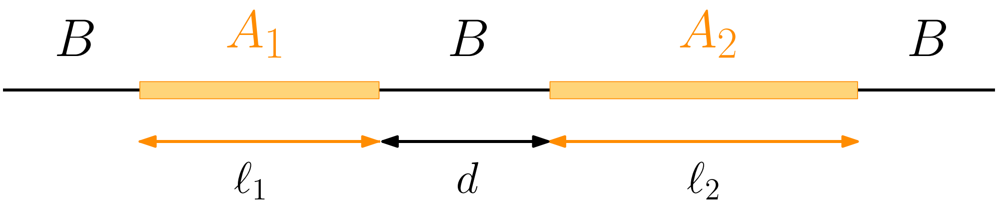

Figure 1. The subsystem A considered consists into two disjoint subsystems A_1 and A_2 of lengths ℓ_1 and ℓ_2, separated by a distance d.

with

$$\begin{aligned}
\epsilon_k^2 &= (h-\cos k)^2+\gamma^2\sin^2 k, \qquad \epsilon_{0,k}^2=(h_0-\cos k)^2+\gamma_0^2\sin^2 k,\\
\mathrm{e}^{-\mathrm{i}\theta_k} &= \frac{\cos k-h-\mathrm{i}\gamma\sin k}{\epsilon_k},\\
\cos\Delta_k &= \frac{hh_0-\cos k(h+h_0)+\cos^2 k+\gamma\gamma_0\sin^2 k}{\epsilon_k\epsilon_{0,k}},\\
\sin\Delta_k &= -\sin k\frac{\gamma h_0-\gamma_0 h-\cos k(\gamma-\gamma_0)}{\epsilon_k\epsilon_{0,k}}.
\end{aligned} \tag{13}$$

2.2. Entanglement entropies and mutual information for disjoint intervals

Owing to the quadratic nature of the XY Hamiltonian in terms of fermion operators, the time-dependent reduced density matrix $\rho_A(t)$ of any subsystem A is a Gaussian operator. This implies that the spectrum of $\rho_A(t)$ is related to the correlation matrix $\Gamma_A(t)$ associated to the same subsystem [63, 64], namely

$$\mathrm{Tr}\rho_A^n=\left(\det\left[\left(\frac{\mathbb{I}+\mathrm{i}\Gamma_A}{2}\right)^n+\left(\frac{\mathbb{I}-\mathrm{i}\Gamma_A}{2}\right)^n\right]\right)^{1/2}, \tag{14}$$

where we removed the explicit time dependence for clarity.

When the subsystem A is a block of contiguous sites, the matrix Γ_A is constructed as in equation (11). However, we are interested in the case of disjoint intervals, where the construction is slightly more subtle. We consider in particular the case where $A=A_1\cup A_2$ consists of two non-complementary subsystems A_1 and A_2 of respective lengths ℓ_1 and ℓ_2 separated by a distance d, as shown in figure 1. Moreover, the length of the total subsystem A is $\ell\equiv\ell_1+\ell_2$. We also mention that, since we work with periodic boundary conditions, one could in principle define two distances d. However, in the following we systematically consider the case where the subsystem A is embedded in an infinite chain $L\to\infty$, and d is the smallest distance between A_1 and A_2.

In this case, the correlation matrix $\Gamma_{A_1\cup A_2}$ has the following block structure,

$$\Gamma_{A_1\cup A_2}=\begin{pmatrix}\Gamma_{11} & \Gamma_{12}\\ \Gamma_{21} & \Gamma_{22}\end{pmatrix}. \tag{15}$$

Here, Γ_{ab}, $a,b=1,2$, are $2\ell_a\times 2\ell_b$ matrices that account for the correlations between subsystems A_a and A_b,

$$
\begin{aligned}
&[\Gamma_{11}]_{j,k} = \Pi_{k-j}, \quad j,k = 1,\ldots,\ell_1, \\
&[\Gamma_{12}]_{j,k} = \Pi_{(k+d+\ell_1)-j}, \quad j = 1,\ldots,\ell_1, \quad k = 1,\ldots,\ell_2, \\
&[\Gamma_{21}]_{j,k} = \Pi_{k-(j+d+\ell_1)}, \quad j = 1,\ldots,\ell_2, \quad k = 1,\ldots,\ell_1, \\
&[\Gamma_{22}]_{j,k} = \Pi_{k-j}, \quad j,k = 1,\ldots,\ell_2,
\end{aligned} \tag{16}
$$

and the 2×2 blocks Π_j are given in equation (11). We note in particular that by definition, $\Gamma_{11} \equiv \Gamma_{A_1}$, and similarly for A_2.

Using equations (14), (1) and (4), we express the Rényi entropies and mutual information for disjoint intervals as

$$
S_n^{A_1\cup A_2} = \frac{1}{2(1-n)}\mathrm{Tr}\log\left[\left(\frac{\mathbb{I}+\mathrm{i}\Gamma_{A_1\cup A_2}}{2}\right)^n + \left(\frac{\mathbb{I}-\mathrm{i}\Gamma_{A_1\cup A_2}}{2}\right)^n\right] \tag{17a}
$$

and

$$
\begin{aligned}
I_n^{A_1:A_2} = &\frac{1}{2(1-n)}\mathrm{Tr}\log\left[\left(\frac{\mathbb{I}+\mathrm{i}\Gamma_{11}}{2}\right)^n + \left(\frac{\mathbb{I}-\mathrm{i}\Gamma_{11}}{2}\right)^n\right] \\
&+ \frac{1}{2(1-n)}\mathrm{Tr}\log\left[\left(\frac{\mathbb{I}+\mathrm{i}\Gamma_{22}}{2}\right)^n + \left(\frac{\mathbb{I}-\mathrm{i}\Gamma_{22}}{2}\right)^n\right] \\
&- \frac{1}{2(1-n)}\mathrm{Tr}\log\left[\left(\frac{\mathbb{I}+\mathrm{i}\Gamma_{A_1\cup A_2}}{2}\right)^n + \left(\frac{\mathbb{I}-\mathrm{i}\Gamma_{A_1\cup A_2}}{2}\right)^n\right].
\end{aligned} \tag{17b}
$$

We mention that the reduced density matrix $\rho_{A_1\cup A_2}$ corresponding to disjoint subsystems is different in the spin-chain picture and in the free-fermion one [32, 34, 35]. This difference arises because of the fermionic string of the Majorana operators and boils down to the fact that the Jordan–Wigner transformation is non-local in terms of the spins. However, in the scaling limit, the entanglement dynamics is identical in both descriptions [42] and hence we do not discuss this issue further.

3. Quasiparticle conjecture for free fermions

The quasiparticle picture is a semiclassical argument that allows one to derive quantitative predictions for the dynamics of entanglement in generic integrable models [27–29, 51, 52]. In this picture, a quantum system is prepared in an initial state that possesses an extensive amount of energy above the ground state of the Hamiltonian determining the time evolution, and hence the initial state acts as source of quasiparticles. The quasiparticles are emitted in pairs with opposite momenta $\pm k$ and move ballistically with a velocity v_k. The fundamental assumption is that quasiparticles emitted from the same point are entangled, and hence spread entanglement and correlations as they propagate. In contrast, quasiparticles emitted from different points are uncorrelated. Accordingly, the amount of entanglement between two subsystems at a given time is proportional to the number of entangled pairs they share.

3.1. Single interval

For a contiguous subsystem A of length ℓ embedded in an infinite system in the scaling limit $\ell, t \to \infty$, with fixed ratio t/ℓ, the entanglement entropy $S_1^A(t)$ is [52]

$$
S_1^A(t) = 2t\int_{2v_k t<\ell}\mathrm{d}k v_k s(k) + \ell\int_{2v_k t>\ell}\mathrm{d}k s(k). \tag{18}
$$

Here, $s(k)$ is a function that depends on the momentum k of each quasiparticle in the pair, and contains all the information on the initial state [29].

In free fermionic systems, the explicit form of $s(k)$ is

$$s(k) = \frac{1}{2\pi}(-n_k \log n_k - (1-n_k)\log(1-n_k)), \tag{19}$$

where n_k is the occupation probability of the mode k in the stationary state. For the Rényi entropy $S_n(t)$, an expression analogous to (18) holds, with

$$s_n(k) = \frac{1}{2\pi}\frac{1}{1-n}\log(n_k^n + (1-n_k^n)) \tag{20}$$

instead of $s(k)$. Introducing the function

$$h_n(x) \equiv \frac{1}{1-n}\log\left[\left(\frac{1+x}{2}\right)^n + \left(\frac{1-x}{2}\right)^n\right], \tag{21}$$

the Rényi entropies can be written as

$$S_n^A(t) = \int \frac{\mathrm{d}k}{2\pi} h_n(2n_k - 1)\min(\ell, 2v_k t). \tag{22}$$

In the case of interacting integrables models, equation (18) needs to include a sum over the different species of quasiparticles [27]. Moreover, in that case it is a hard problem to derive the function $s(k)$, and the quasiparticle picture breaks down for Rényi entropies with $n \neq 1$, i.e. the simple prescription of equation (20) does not hold.

In the XY chain, equation (22) becomes [26]

$$S_n^A(t) = \int_{-\pi}^{\pi} \frac{\mathrm{d}k}{2\pi} h_n(\cos\Delta_k)\min(\ell, 2v_k t), \tag{23}$$

where $v_k = |\epsilon_k'|$, and $\cos\Delta_k, \epsilon_k$ are defined in equation (13). The quasiparticle conjecture of equation (23) is proved in [26].

3.2. Two disjoint intervals

The quasiparticle picture also allows one to predict the time evolution of the entanglement between two disjoint blocks A_1 and A_2 [41, 42] of lengths ℓ_1, ℓ_2 and separated by a distance d, as illustrated in figure 1. As for the case of one block, the entanglement between the two disjoint blocks is proportional to the number of shared pairs of quasiparticles over time. The counting exercise that leads to equation (18) is modified by the presence of the two intervals, but its generalization is standard. The subsystem $A = A_1 \cup A_2$ is embedded in an infinite chain, and we work in the scaling limit $\ell_1, \ell_2, d, t \to \infty$ with fixed ratios $\ell_1/\ell, \ell_2/\ell, d/\ell$ and t/ℓ, where $\ell = \ell_1 + \ell_2$. Moreover, we introduce the function

$$\Xi_{\ell_1,\ell_2,d,t}(k) = \max(d, 2v_k t) + \max(d+\ell, 2v_k t) - \max(d+\ell_1, 2v_k t) - \max(d+\ell_2, 2v_k t). \tag{24}$$

For free fermionic systems, the Rényi mutual information reads [42]

$$I_n^{A_1:A_2}(t) = \int \frac{\mathrm{d}k}{2\pi} h_n(2n_k - 1)\Xi_{\ell_1,\ell_2,d,t}(k), \tag{25}$$

where $h_n(x)$ is defined in (21). We mention that the quench dynamics of logarithmic negativity can also be described by the quasiparticle picture [42], and the result is similar to equation (25).

In the XY chain, the quasiparticle conjecture of equation (25) reads

$$I_n^{A_1:A_2}(t) = \int_{-\pi}^{\pi} \frac{\mathrm{d}k}{2\pi} h_n(\cos\Delta_k)\Xi_{\ell_1,\ell_2,d,t}(k). \tag{26}$$

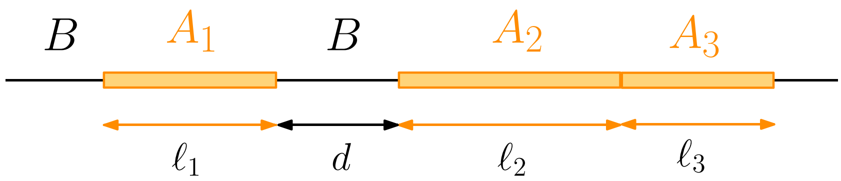

Figure 2. The tripartite subsystem A consists into three subsystems, A_1 and A_2 which are separated by a distance d, and A_3 that is adjacent to A_2.

3.3. Three intervals

We consider the case where $A = A_1 \cup A_2 \cup A_3$ consists of three intervals of lengths ℓ_1, ℓ_2, ℓ_3 with $\ell_1 + \ell_2 + \ell_3 = \ell$. For simplicity, we assume that A_1 and A_2 are separated by a distance d, but A_2 and A_3 are adjacent. This geometry is illustrated in figure 2. Combining equations (5) and (25), we find

$$I_n^{A_1:A_2:A_3}(t) = \int \frac{\mathrm{d}k}{2\pi} h_n(2n_k - 1)(\Xi_{\ell_1,\ell_2,d,t}(k) + \Xi_{\ell_1,\ell_3,d+\ell_2,t}(k) - \Xi_{\ell_1,\ell_2+\ell_3,d,t}(k)) = 0 \quad (27)$$

in the scaling limit where the lengths and time are infinite, but all the ratios are fixed. This simple calculation shows that, for free systems, the tripartite information for the geometry of figure 2 vanishes for all values of t/ℓ in the scaling limit. In particular, equation (27) holds for the XY chain. A direct generalization of equation (27) with $s(k)$ instead of $h_n(2n_k - 1)$, and a sum over the different species of quasiparticles, implies that the tripartite information $I_1^{A_1:A_2:A_3}(t)$ vanishes identically for all interacting integrable systems.

3.4. Conjecture for the Rényi entropies of disjoint blocks in the XY chain

In the case of two disjoint intervals, combining equations (23), (26) and (4), and using the fact that A_1 and A_2 are both contiguous blocks, the quasiparticle conjecture for the Rényi entropies reads [32]

$$S_n^{A_1 \cup A_2}(t) = \int_{-\pi}^{\pi} \frac{\mathrm{d}k}{2\pi} h_n(\cos\Delta_k)[\min(\ell_1, 2v_k t) + \min(\ell_2, 2v_k t) - \Xi_{\ell_1,\ell_2,d,t}(k)]. \quad (28)$$

It is direct to check that equation (28) reduces to equation (23) for $d = 0$, as expected. In the following, we prove equation (28), and hence equations (26) and (27) too, as byproducts.

3.5. Numerical checks

In this section, we compare the quasiparticle results of equations (28) and (26) with numerical results that rely on the exact diagonalization of the correlation matrices from equations (11) and (15) inserted in equation (17). We show this comparison in figure 3 for $S_1^{A_1 \cup A_2}(t)$, $S_2^{A_1 \cup A_2}(t)$, $I_1^{A_1:A_2}(t)$ and $I_2^{A_1:A_2}(t)$ as a function of t/ℓ for fixed $d/\ell, \ell_1/\ell$ and quench parameters γ_0, h_0, γ, h. The solid lines are the quasiparticle results, whereas the symbols are the numerical ones for different values of ℓ. The agreement is better for the mutual information, but the results for the entropies is convincing too, and it is in particular clear that the quasiparticle result is exact in the scaling limit, as expected.

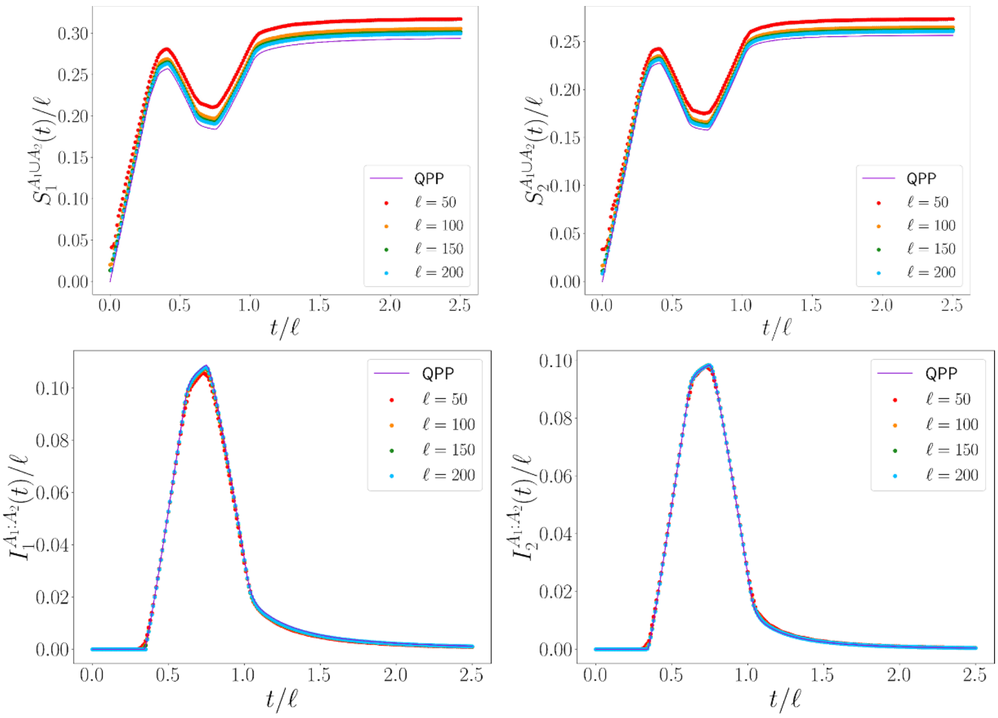

Figure 3. Entanglement entropies $S_1^{A_1\cup A_2}(t)$ and $S_2^{A_1\cup A_2}(t)$ (top) and mutual information $I_1^{A_1:A_2}(t)$ and $I_2^{A_1:A_2}(t)$ (bottom) as a function of t/ℓ for various values of ℓ with $\ell_1/\ell = 0.4$ and $d/\ell = 0.5$. The quench parameters are $h_0 = 0.1$, $\gamma_0 = 0.2$, $h = 0.8$ and $\gamma = 0.9$. The solid lines are the quasiparticle predictions of equation (28) (top) and equation (26) (bottom), and the symbols are obtained by exact diagonalization of the correlation matrices and equation (17).

4. Proof of the quasiparticle conjecture for two disjoint blocks

In this section, we adapt the methods developed in [26] to prove equation (28). The initial step is to recast equation (17*a*) as a series. We introduce the Taylor expansion of the function $h_n(x)$,

$$h_n(x) = \sum_{j=0}^{\infty} c_n(2j)x^{2j}, \tag{29}$$

and find

$$S_n^{A_1\cup A_2}(t) = \frac{1}{2}\sum_{j=0}^{\infty} c_n(2j)\mathrm{Tr}(\mathrm{i}\Gamma_{A_1\cup A_2}(t))^{2j}. \tag{30}$$

We mention that the series in equation (29) contains only even powers, because $h_n(x) = h_n(-x)$, and $h_n(x)$ is defined in equation (21).

In the following, we thus focus on the computation of $\mathrm{Tr}(\mathrm{i}\Gamma_{A_1\cup A_2}(t))^{2j}$. For further convenience, we recast this trace as

$$\mathrm{Tr}(\mathrm{i}\Gamma_{A_1\cup A_2}(t))^{2j} \equiv \mathrm{Tr}(\mathrm{i}\Gamma_{11}(t))^{2j} + \mathrm{Tr}(\mathrm{i}\Gamma_{22}(t))^{2j} + T_{2j}(t), \tag{31}$$

where we used the block structure described in equation (15), and $T_{2j}(t)$ is a non-trivial combination of traces of products of $2j$ matrices from the set $\{\Gamma_{11}(t), \Gamma_{12}(t), \Gamma_{21}(t), \Gamma_{22}(t)\}$.

In the geometry we consider, both A_1 and A_2 are contiguous blocks of respective lengths ℓ_1 and $\ell_2 = \ell - \ell_1$, and their respective associated correlation matrices are Γ_{11} and Γ_{22}. Hence the results of [26] directly apply to the first two terms of the right-hand side of equation (31). In the scaling limit $\ell_1, \ell_2, t \to \infty$ with fixed ratios $\ell_1/\ell, \ell_2/\ell$ and t/ℓ, we thus have

$$\mathrm{Tr}(\mathrm{i}\Gamma_{11}(t))^{2j} + \mathrm{Tr}\,(\mathrm{i}\Gamma_{22}(t))^{2j} = 2\ell - 2\int \frac{\mathrm{d}k}{2\pi}\left(1-(\cos\Delta_k)^{2j}\right)[\min(\ell_1, 2v_k t) + \min(\ell_2, 2v_k t)] \tag{32}$$

where we recall $v_k = |\epsilon_k'|$.

It remains to investigate the term $T_{2j}(t)$ from equation (31) in the scaling limit $\ell_1, \ell_2, d, t \to \infty$ with fixed ratios $\ell_1/\ell, \ell_2/\ell, d/\ell$ and t/ℓ. As expected, this term contains non-trivial dependence on the three lengths ℓ_1, ℓ_2 and d.

4.1. Calculation of $T_2(t)$

For simplicity, we begin with the calculation of $T_2(t)$. We have

$$\begin{aligned} T_2 &= -2\mathrm{Tr}(\Gamma_{12}\Gamma_{21}) \\ &= 2\sum_{m_1=1}^{\ell_1}\sum_{m_2=1}^{\ell_2}\left(2f^2_{(m_2+\ell_1+d)-m_1} + g^2_{(m_2+\ell_1+d)-m_1} + g^2_{m_1-(m_2+\ell_1+d)}\right) \end{aligned} \tag{33}$$

where we used equations (11) and (16), as well as $f_{-j} = -f_j$. In the notations, we dropped the explicit time dependence for clarity.

4.1.1. Summation formulas.

First, we focus on terms of the form f_j^2 in equation (33). With equation (12), we find

$$f^2{}_{(m_2+\ell_1+d)-m_1} = \int_{-\pi}^{\pi}\int_{-\pi}^{\pi}\frac{\mathrm{d}k_1\mathrm{d}k_2}{4\pi^2}\mathrm{e}^{-\mathrm{i}(k_1-k_2)(m_2-m_1+\ell_1+d)}\sin\Delta_{k_1}\sin\Delta_{k_2}\sin(2\epsilon_{k_1}t)\sin(2\epsilon_{k_2}t). \tag{34}$$

With the identity

$$\sum_{m=1}^{\ell}\mathrm{e}^{\mathrm{i}km} = \mathrm{e}^{\mathrm{i}k\left(\frac{\ell+1}{2}\right)}\frac{\sin\left(\frac{\ell}{2}k\right)}{\sin\left(\frac{k}{2}\right)}, \tag{35}$$

we obtain

$$\begin{aligned} \sum_{m_1=1}^{\ell_1}\sum_{m_2=1}^{\ell_2} f^2{}_{(m_2+\ell_1+d)-m_1} &= \int_{-\pi}^{\pi}\int_{-\pi}^{\pi}\frac{\mathrm{d}k_1\mathrm{d}k_2}{4\pi^2}\sin\Delta_{k_1}\sin\Delta_{k_2}\sin(2\epsilon_{k_1}t)\sin(2\epsilon_{k_2}t) \\ &\quad\times\left[\mathrm{e}^{-\mathrm{i}(k_1-k_2)\left(\frac{\ell_1}{2}+\frac{\ell_2}{2}+d\right)}\frac{\sin\left(\frac{\ell_1}{2}(k_1-k_2)\right)\sin\left(\frac{\ell_2}{2}(k_1-k_2)\right)}{\sin^2\left(\frac{(k_1-k_2)}{2}\right)}\right]. \end{aligned} \tag{36}$$

Second, we consider terms of the form g_j^2 in equation (33). We introduce

$$\eta(k) = \cos\Delta_k + \mathrm{i}\sin\Delta_k\cos(2\epsilon_k t) \tag{37}$$

and find

$$g^2_{(m_2+\ell_1+d)-m_1} = \int_{-\pi}^{\pi}\int_{-\pi}^{\pi}\frac{\mathrm{d}k_1\mathrm{d}k_2}{4\pi^2}\mathrm{e}^{-\mathrm{i}(k_1-k_2)(m_2-m_1+\ell_1+d)}\mathrm{e}^{-\mathrm{i}(\theta_{k_1}-\theta_{k_2})}\eta(k_1)\eta^*(k_2), \tag{38}$$

where we used $\eta(k)=\eta^*(-k)$. Using equation (35), we obtain

$$\sum_{m_1=1}^{\ell_1}\sum_{m_2=1}^{\ell_2} g^2_{(m_2+\ell_1+d)-m_1} = \int_{-\pi}^{\pi}\int_{-\pi}^{\pi}\frac{\mathrm{d}k_1\mathrm{d}k_2}{4\pi^2}\mathrm{e}^{-\mathrm{i}(\theta_{k_1}-\theta_{k_2})}\eta(k_1)\eta^*(k_2) \times\left[\mathrm{e}^{-\mathrm{i}(k_1-k_2)\left(\frac{\ell_1}{2}+\frac{\ell_2}{2}+d\right)}\frac{\sin\left(\frac{\ell_1}{2}(k_1-k_2)\right)\sin\left(\frac{\ell_2}{2}(k_1-k_2)\right)}{\sin^2\left(\frac{k_1-k_2}{2}\right)}\right]. \quad (39a)$$

Similarly, we find

$$\sum_{m_1=1}^{\ell_1}\sum_{m_2=1}^{\ell_2} g^2_{m_1-(m_2+\ell_1+d)} = \int_{-\pi}^{\pi}\int_{-\pi}^{\pi}\frac{\mathrm{d}k_1\mathrm{d}k_2}{4\pi^2}\mathrm{e}^{\mathrm{i}(\theta_{k_1}-\theta_{k_2})}\eta^*(k_1)\eta(k_2) \times\left[\mathrm{e}^{-\mathrm{i}(k_1-k_2)\left(\frac{\ell_1}{2}+\frac{\ell_2}{2}+d\right)}\frac{\sin\left(\frac{\ell_1}{2}(k_1-k_2)\right)\sin\left(\frac{\ell_2}{2}(k_1-k_2)\right)}{\sin^2\left(\frac{k_1-k_2}{2}\right)}\right]. \quad (39b)$$

To proceed, we use the following identity in equations (36) and (39),

$$\frac{\sin\left(\frac{\ell}{2}(k_1-k_2)\right)}{\sin\left(\frac{k_1-k_2}{2}\right)} = \frac{\ell}{2}\frac{\left(\frac{k_1-k_2}{2}\right)}{\sin\left(\frac{k_1-k_2}{2}\right)}\int_{-1}^{1}\mathrm{d}\zeta\cos\left(\frac{\ell\zeta}{2}(k_1-k_2)\right). \quad (40)$$

Moreover, we replace $\mathrm{e}^{\pm\mathrm{i}(\theta_{k_1}-\theta_{k_2})}$ and $2\sin\left(\frac{k_1-k_2}{2}\right)/(k_1-k_2)$ by one in the integrals, because they do not depend on ℓ, t, and we anticipate that they are evaluated at $k_1=k_2$ in the stationary phase approximation. Finally, the purely imaginary terms arising from the products $\eta^*(k_1)\eta(k_2)$ and $\eta(k_1)\eta^*(k_2)$ in the integrals vanish by symmetry. We thus find

$$T_2 = \ell_1\ell_2\int_{-\pi}^{\pi}\int_{-\pi}^{\pi}\frac{\mathrm{d}k_1\mathrm{d}k_2}{4\pi^2}\int_{-1}^{1}\int_{-1}^{1}\mathrm{d}\zeta_1\mathrm{d}\zeta_2\mathrm{e}^{-\mathrm{i}(k_1-k_2)\left(\frac{\ell}{2}+d\right)} \times\cos\left(\frac{\ell_1\zeta_1}{2}(k_1-k_2)\right)\cos\left(\frac{\ell_2\zeta_2}{2}(k_1-k_2)\right)\mathcal{B}_2(k_1,k_2), \quad (41)$$

where

$$\mathcal{B}_2(k_1,k_2) = \cos\Delta_{k_1}\cos\Delta_{k_2}+\sin\Delta_{k_1}\sin\Delta_{k_2}\cos(2\epsilon_{k_1}t-2\epsilon_{k_2}t). \quad (42)$$

4.1.1.1. Integrals over ζ. Let us focus on the integrals over ζ_1, ζ_2,

$$Z_2 \equiv \int_{-1}^{1}\int_{-1}^{1}\mathrm{d}\zeta_1\mathrm{d}\zeta_2\cos\left(\frac{\ell_1\zeta_1}{2}(k_1-k_2)\right)\cos\left(\frac{\ell_2\zeta_2}{2}(k_1-k_2)\right). \quad (43)$$

Because the integrals are symmetric about $\zeta_{1,2}=0$ and the kernel is invariant under $\zeta_{1,2}\to-\zeta_{1,2}$, we have

$$Z_2 = \int_{-1}^{1}\int_{-1}^{1}\mathrm{d}\zeta_1\mathrm{d}\zeta_2\cos\left(\frac{\ell}{2}(x_2\zeta_2-x_1\zeta_1)(k_1-k_2)\right) \quad (44)$$

with $x_j=\ell_j/\ell$, $j=1,2$. We introduce the change of variables

$$\rho_0 = x_1\zeta_1$$
$$\rho_1 = x_2\zeta_2-x_1\zeta_1, \quad (45)$$

and obtain

$$Z_2 = \frac{\ell^2}{\ell_1\ell_2}\int_{-x_1}^{x_1}\mathrm{d}\rho_0\int_{-x_2-\rho_0}^{x_2-\rho_0}\mathrm{d}\rho_1\cos\left(\frac{\ell}{2}\rho_1(k_1-k_2)\right). \quad (46)$$

The bounds of integration depend on ρ_0, whereas the kernel do not, and it is possible to reduce this double integral as a single integral over ρ_1. For a generic function $J(\rho_1)$, we have

$$\int_{-x_1}^{x_1} \mathrm{d}\rho_0 \int_{-x_2-\rho_0}^{x_2-\rho_0} \mathrm{d}\rho_1 J(\rho_1) = \int_{\mathbb{R}} \mathrm{d}\rho_1 J(\rho_1)\Omega_{12}(\rho_1), \tag{47a}$$

where

$$\Omega_{12}(\rho_1) = \max[0, \min(x_1, x_2+\rho_1) + \min(x_1, x_2-\rho_1)]. \tag{47b}$$

We stress that equation (47) is a non-trivial generalization of a similar result used in [26] for the case of a single block.

Combining equations (41), (46) and (47), we find

$$T_2 = \frac{\ell^2}{2\pi}\int_{-\pi}^{\pi}\frac{\mathrm{d}k}{2\pi}\left[\int_{[-\pi,\pi]\times\mathbb{R}} \mathrm{d}k_1 \mathrm{d}\rho_1 \mathrm{e}^{-\mathrm{i}(k_1-k)\left(\frac{\ell}{2}+d\right)}\mathcal{B}_2(k_1,k)\mathrm{e}^{\frac{\mathrm{i}\ell\rho_1}{2}(k_1-k)}\Omega_{12}(\rho_1)\right] \tag{48}$$

where we used the symmetry about 0 of the integral over ρ_1 to replace $\cos\left(\frac{\ell}{2}\rho_1(k_1-k_2)\right)$ by an exponential.

4.1.1.2. Multidimensional stationary phase approximation. We study the asymptotic behaviour of the two-fold integral over k_1 and ρ_1 in equation (48) using multidimensional stationary phase approximation. This method can be used to evaluate integrals of the form

$$I(\ell) = \int_{\mathbb{R}^n} \mathrm{d}x\, G(x)\mathrm{e}^{\mathrm{i}\ell F(x)}, \tag{49}$$

in the limit $\ell \to \infty$. In the case where there is only one point $x_0 \in \mathbb{R}^n$ such that $\nabla F(x_0) = 0$, we have

$$\lim_{\ell\to\infty} I(\ell) = G(x_0)\mathrm{e}^{\mathrm{i}\ell F(x_0)}\left(\frac{2\pi}{\ell}\right)^{\frac{n}{2}} |\det \mathrm{Hess}(F(x_0))|^{-\frac{1}{2}} + o(\ell^{-\frac{n}{2}}). \tag{50}$$

Using the definition (42) of $\mathcal{B}_2$, the integral in equation (48) has two distinct terms, one is time-independent, and the second contains all the time dependence. We study these two terms separately.

For the time-independent term, the two-fold integral can be written in the form of equation (49) with

$$\begin{aligned} F(k_1,\rho_1) &= -(k_1-k)\left(\frac{1}{2}+\frac{d}{\ell}\right) + \frac{\rho_1}{2}(k_1-k), \\ G(k_1,\rho_1) &= \cos\Delta_{k_1}\cos\Delta_k\Omega_{12}(\rho_1). \end{aligned} \tag{51}$$

The stationary point is $x_0 = (k, 1+\frac{2d}{\ell})$. It is direct to verify that $\Omega_{12}(1+\frac{2d}{\ell}) = 0$, and hence the time-independent term does not contribute in the scaling limit.

For the time dependent term, we write $\cos(2\epsilon_{k_1}t - 2\epsilon_{k_2}t)$ from $\mathcal{B}_2$ in exponential form, and hence we have two terms with opposite phases. Both integrals have the form of equation (49) with

$$F_t(k_1,\rho_1) = -(k_1-k)\left(\frac{1}{2}+\frac{d}{\ell}\right) + \frac{\rho_1}{2}(k_1-k) \pm \frac{2t}{\ell}(\epsilon_{k_1}-\epsilon_k),$$
$$G_t(k_1,\rho_1) = \sin\Delta_{k_1}\sin\Delta_k\Omega_{12}(\rho_1). \tag{52}$$

The stationary points are $x_0 = (k, 1+\frac{2d}{\ell}\mp\frac{4t}{\ell}\epsilon_k')$. We have $|\det\mathrm{Hess}(F_t(x_0))| = 2^{-2}$, and hence equations (50) and (48) yield

$$T_2(t) = \ell\int_{-\pi}^{\pi}\frac{\mathrm{d}k}{2\pi}(1-(\cos\Delta_k)^2)\left[\Omega_{12}\Big(1+\frac{2d}{\ell}+\frac{4t}{\ell}\epsilon_k'\Big)+\Omega_{12}\Big(1+\frac{2d}{\ell}-\frac{4t}{\ell}\epsilon_k'\Big)\right]. \tag{53}$$

Similarly as for the time-independent term, $\Omega_{12}\Big(1+\frac{2d}{\ell}+a\Big) = 0$ for $a\geqslant 0$, and hence we recast $T_2(t)$ as

$$T_2(t) = \ell\int_{-\pi}^{\pi}\frac{\mathrm{d}k}{2\pi}(1-(\cos\Delta_k)^2)\Omega_{12}\Big(1+\frac{2d}{\ell}-\frac{4t}{\ell}v_k\Big) \tag{54}$$

with $v_k = |\epsilon_k'|$. A direct calculation gives $\Omega_{12}\Big(1+\frac{2d}{\ell}-\frac{4t}{\ell}v_k\Big) = 2/\ell\ \Xi_{\ell_1,\ell_2,d,t}(k)$, where $\Xi_{\ell_1,\ell_2,d,t}(k)$ is defined in (24), and hence we conclude

$$T_2(t) = 2\int_{-\pi}^{\pi}\frac{\mathrm{d}k}{2\pi}(1-(\cos\Delta_k)^2)\ \Xi_{\ell_1,\ell_2,d,t}(k). \tag{55}$$

4.2. Calculation of $T_{2j}(t)$

In this section, we generalize the calculations of the previous one to the case of $T_{2j}(t)$, where j is a positive integer, and we recall that $T_{2j}(t)$ is defined in equation (32). It is a sum of traces of various combinations of products of Γ_{ab} matrices. For convenience, we first focus on one certain type of sets of matrices Γ_{ab}, namely

$$\Gamma_{r,l,j} = \{\underbrace{\Gamma_{12},\Gamma_{21}}_{r-1\ \text{times}},\Gamma_{12},\underbrace{\Gamma_{22},\ldots,\Gamma_{22}}_{2j-2r-l\ \text{times}},\Gamma_{21},\underbrace{\Gamma_{11},\ldots,\Gamma_{11}}_{l\ \text{times}}\} \tag{56}$$

where r, l are positive integers that satisfy $r > 0$ and $2j-2r-l\geqslant 0$. The matrix at position $i = 1,\ldots,2j$ in the set $\Gamma_{r,l,j}$ is $\Gamma_{a_ib_i}$. We also define $X_{r,l,j}$ as the set where the entry at position $i = 1,\ldots,2j$ is the ratio $X_{r,l,j}(i) = \ell_{a_i}/\ell$. Finally, introduce the quantity $C_{r,l,j}$ as the trace of the product of all the matrices in $\mathrm{i}\Gamma_{r,l,j}$,

$$C_{r,l,j} \equiv (-1)^j\mathrm{Tr}[(\Gamma_{12}\Gamma_{21})^{r-1}\Gamma_{12}\Gamma_{22}^{2j-2r-l}\Gamma_{21}\Gamma_{11}^l], \tag{57}$$

where we introduced the sign $(-1)^j = \mathrm{i}^{2j}$, because in the definition of T_{2j}, all the Γ_{ab} matrices are multiplied by i. As an example, for $r = 2, l = 1, j = 3$, we have

$$\Gamma_{2,1,3} = \{\Gamma_{12},\Gamma_{21},\Gamma_{12},\Gamma_{22},\Gamma_{21},\Gamma_{11}\},$$
$$X_{2,1,3} = \left\{\frac{\ell_1}{\ell},\frac{\ell_2}{\ell},\frac{\ell_1}{\ell},\frac{\ell_2}{\ell},\frac{\ell_2}{\ell},\frac{\ell_1}{\ell}\right\},$$
$$C_{2,1,3} = -\mathrm{Tr}[\Gamma_{12}\Gamma_{21}\Gamma_{12}\Gamma_{22}\Gamma_{21}\Gamma_{11}]. \tag{58}$$

4.2.1. Computation of $C_{r,l,j}$. Using similar calculation as in the previous section, we find

$$C_{r,l,j} = \frac{\ell_1^{r+l}\ell_2^{2j-r-l}}{2^{2j-1}} \int \left(\prod_{i=1}^{2j} \frac{\mathrm{d}k_i}{2\pi}\right)\left(\prod_{i=1}^{2j}\mathrm{d}\zeta_i\right) \mathrm{e}^{\mathrm{i}\left(\frac{\ell}{2}+d\right)\left(\sum_{i=1}^{2r-1}(-1)^i k_i + k_{2j-l}\right)} \times \mathcal{B}_{2j}\prod_{i=1}^{2j}\cos\left(\frac{\ell}{2}x_i\zeta_i(k_i-k_{i-1})\right), \tag{59}$$

where $x_i = X_{r,l,j}(i)$, see previous paragraph, and we assume a periodicity of $2j$ in the indices, namely $k_0 = k_{2j}$. The function $\mathcal{B}_{2j}$ is a non-trivial generalization of the B function from [26]. We consider the set of integers $\lambda^{(2j)} = \{1,2,\ldots,2j\}$, and we denote by $\lambda_{2p}^{(2j)} \in \lambda^{(2j)}$ a subset which contains $2p \leqslant 2j$ of these integers, and $\bar{\lambda}_{2p}^{(2j)}$ is its complement, $\lambda_{2p}^{(2j)} \cup \bar{\lambda}_{2p}^{(2j)} = \lambda^{(2j)}$. We impose that both sets are ordered, namely their elements are strictly increasing. Moreover, for $i \in \lambda_{2p}^{(2j)}$, the function $s(i)$ gives the position of i in the set. For example, for $j=2$, one choice of subset is $\lambda_2^{(4)} = \{2,3\}$, and we have $s(2)=1$ and $s(3)=2$. With these definitions, we find

$$\mathcal{B}_{2j} = \sum_{p=0}^{j}\sum_{\lambda_{2p}^{(2j)}}(-1)^{|\lambda_{2p}^{(2j)}|+p}\left[\cos\left(2t\sum_{u\in\lambda_{2p}^{(2j)}}(-1)^{s(u)}\epsilon_{k_u}\right)\prod_{u\in\lambda_{2p}^{(2j)}}\sin\Delta_{k_u}\prod_{v\in\bar{\lambda}_{2p}^{(2j)}}\cos\Delta_{k_v}\right] \tag{60}$$

with $|\lambda_{2p}^{(2j)}| = \sum_{i\in\lambda_{2p}^{(2j)}} i$. As examples, $\mathcal{B}_2$ is given in equation (42), and $\mathcal{B}_4$ is

$$\begin{aligned}
\mathcal{B}_4 = {} & \cos\Delta_{k_1}\cos\Delta_{k_2}\cos\Delta_{k_3}\cos\Delta_{k_4}\\
& + \cos(2t(\epsilon_{k_1}-\epsilon_{k_2}))\sin\Delta_{k_1}\sin\Delta_{k_2}\cos\Delta_{k_3}\cos\Delta_{k_4}\\
& - \cos(2t(\epsilon_{k_1}-\epsilon_{k_3}))\sin\Delta_{k_1}\sin\Delta_{k_3}\cos\Delta_{k_2}\cos\Delta_{k_4}\\
& + \cos(2t(\epsilon_{k_1}-\epsilon_{k_4}))\sin\Delta_{k_1}\sin\Delta_{k_4}\cos\Delta_{k_2}\cos\Delta_{k_3}\\
& + \cos(2t(\epsilon_{k_2}-\epsilon_{k_3}))\sin\Delta_{k_2}\sin\Delta_{k_3}\cos\Delta_{k_1}\cos\Delta_{k_4}\\
& - \cos(2t(\epsilon_{k_2}-\epsilon_{k_4}))\sin\Delta_{k_2}\sin\Delta_{k_4}\cos\Delta_{k_1}\cos\Delta_{k_3}\\
& + \cos(2t(\epsilon_{k_3}-\epsilon_{k_4}))\sin\Delta_{k_3}\sin\Delta_{k_4}\cos\Delta_{k_1}\cos\Delta_{k_2}\\
& + \cos(2t(\epsilon_{k_1}-\epsilon_{k_2}+\epsilon_{k_3}-\epsilon_{k_4}))\sin\Delta_{k_1}\sin\Delta_{k_2}\sin\Delta_{k_3}\sin\Delta_{k_4}.
\end{aligned} \tag{61}$$

Going back to equation (59), using the symmetry about 0 of the ζ_i integrals, we transform the product of cosines into the cosine of a sum as follows

$$\prod_{i=1}^{2j}\cos\left(\frac{\ell}{2}x_i\zeta_i(k_i-k_{i-1})\right) = \cos\left(\frac{\ell}{2}\sum_{i=1}^{2j-1}(x_{i+1}\zeta_{i+1}-x_i\zeta_i)(k_i-k_{2j})\right). \tag{62}$$

We stress that this equation is not an identity and only holds in the integrals. To proceed, we introduce the change of variables

$$\begin{aligned}
\rho_0 &= x_1\zeta_1\\
\rho_i &= x_{i+1}\zeta_{i+1} - x_i\zeta_i, \qquad i = 1,\ldots,2j-1,
\end{aligned} \tag{63}$$

and obtain

$$C_{r,l,j} = \ell \left(\frac{\ell}{2}\right)^{2j-1} \int \left(\prod_{i=1}^{2j} \frac{\mathrm{d}k_i}{2\pi}\right) \left(\prod_{i=0}^{2j-1} \mathrm{d}\rho_i\right) \mathrm{e}^{\mathrm{i}\left(\frac{\ell}{2}+d\right)\left(\sum_{i=1}^{2r-1}(-1)^i k_i + k_{2j-l}\right)} \times \mathcal{B}_{2j} \cos\left(\frac{\ell}{2}\sum_{i=1}^{2j-1} \rho_i (k_i - k_{2j})\right). \tag{64}$$

Here, the integral over ρ_i is between $\left(-x_{i+1} - \sum_{m=0}^{i-1}\rho_m\right)$ and $\left(x_{i+1} - \sum_{m=0}^{i-1}\rho_m\right)$. Similarly as for the case $j = 1$, the kernel does not depend on ρ_0, and we have

$$C_{r,l,j} = \ell \left(\frac{\ell}{4\pi}\right)^{2j-1} \int_{-\pi}^{\pi} \frac{\mathrm{d}k}{2\pi} \left[\int_{[-\pi,\pi]^{2j-1}\times\mathbb{R}^{2j-1}} \left(\prod_{i=1}^{2j-1} \mathrm{d}k_i \mathrm{d}\rho_i\right) \times \mathrm{e}^{\mathrm{i}\left(\frac{\ell}{2}+d\right)\left(\sum_{i=1}^{2r-1}(-1)^i k_i + k_{2j-l}\right)} \mathcal{B}_{2j} \cos\left(\frac{\ell}{2}\sum_{i=1}^{2j-1}\rho_i(k_i - k)\right) \Omega_{12}(\{\rho_i\})\right], \tag{65}$$

where we set $k_{2j} \equiv k$, and

$$\Omega_{12}(\{\rho_i\}) = \max\left[0, \min_{w=1,\ldots,2j-1}\left(x_1, x_{w+1} + \sum_{m=1}^{w}\rho_m\right) + \min_{w=1,\ldots,2j-1}\left(x_1, x_{w+1} - \sum_{m=1}^{w}\rho_m\right)\right]. \tag{66}$$

We treat the $(4j-2)$-fold integral in equation (65) using the multidimensional stationary phase approximation discussed in the previous section. Crucially, the only term in $\mathcal{B}_{2j}$ that contributes in the scaling limit is the one where the time-dependent factor contains energies whose signs and indices match those of the k_i in the overall the phase $\mathrm{e}^{\mathrm{i}\left(\frac{\ell}{2}+d\right)\left(\sum_{i=1}^{2r-1}(-1)^i k_i + k_{2j-l}\right)}$ in equation (65). This time-dependent term is $(-1)^l \cos\left(2t\sum_{i=1}^{2r-1}(-1)^i\epsilon_{k_i} + 2t\epsilon_{k_{2j-l}}\right)(\cos\Delta_k)^{2j-2r}(\sin\Delta_k)^{2r}$, where we anticipated that all the momenta are evaluated at $k_i = k$ in the stationary phase approximation. The sign $(-1)^l$ is a direct consequence of the definition of $\mathcal{B}_{2j}$, see equation (60). The stationary phase calculation is similar to the case $j = 1$, and we find

$$C_{r,l,j} = (-1)^l \int_{-\pi}^{\pi} \frac{\mathrm{d}k}{2\pi} (\cos\Delta_k)^{2j-2r}(\sin\Delta_k)^{2r}\Xi_{\ell_1,\ell_2,d,t}(k). \tag{67}$$

4.2.2. Reconstruction of $T_{2j}(t)$. Thus far, we have investigated the scaling behaviour of a very specific type of trace of product of Γ_{ab} matrices, namely the quantity $C_{r,l,j}$ defined in equation (57). Of course, in T_{2j}, there are many more contributions, arising from different ways of arranging the Γ_{ab} matrices. However, in the scaling limit, the traces of products of matrices taken from a same set but arranged in different orders are equal. We stress that this is not true in finite size, because the blocks of the matrices do not commute. Hence, in the scaling limit, we can write the general formula

$$T_{2j} = \sum_{r=1}^{j}\sum_{l=0}^{2j-2r} \alpha_{r,l,j} C_{r,l,j}, \tag{68}$$

where $\alpha_{r,l,j}$ is the number of ways of arranging the matrices from the set $\Gamma_{r,l,j}$ defined in equation (56) such that the resulting product is a square matrix of size $\ell_1 \times \ell_1$ or $\ell_2 \times \ell_2$. A simple combinatorial argument yields

$$\alpha_{r,l,j} = \frac{2rj}{(2j-r-l)(r+l)} \binom{2j-r-l}{r} \binom{r+l}{r}. \tag{69}$$

Crucially, the coefficients $\alpha_{r,l,j}$ satisfy [55, 65]

$$\sum_{l=0}^{2j-2r} (-1)^l \alpha_{r,l,j} = 2\binom{j}{r}. \tag{70}$$

Finally, using the binomial relation

$$\sum_{r=1}^{j} \binom{j}{r} (\cos\Delta_k)^{2j-2r} (\sin\Delta_k)^{2r} = 1 - (\cos\Delta_k)^{2j} \tag{71}$$

together with equations (67), (68) and (70), we get

$$T_{2j}(t) = 2\int \frac{\mathrm{d}k}{2\pi}(1-(\cos\Delta_k)^{2j})\Xi_{\ell_1,\ell_2,d,t}(k) \tag{72}$$

in the scaling limit. This result appears to be a straightforward generalization of equation (55), but the proof is not.

4.3. Final resummation and conclusion of the proof

To conclude the proof, we need to perform the resummation of equation (30). First, we note that since $h_n(1) = 0$, the sum of all the Taylor coefficients vanishes, $\sum_{j=0}^{\infty} c_n(2j) = 0$. Hence, the terms that do not depend on the summation index j in the quantities we sum over do not contribute. Combining equations (29)–(32) and (72), we find

$$S_n^{A_1\cup A_2}(t) = \int_{-\pi}^{\pi} \frac{\mathrm{d}k}{2\pi} h_n(\cos\Delta_k)[\min(\ell_1, 2v_k t) + \min(\ell_2, 2v_k t) - \Xi_{\ell_1,\ell_2,d,t}(k)], \tag{73}$$

as claimed in section 3.4, equation (28).

As advertised, a direct corollary is that equation (26) holds for the mutual information. Indeed, following the same strategy as for the entropies of disjoint blocks, we have

$$\begin{aligned} I_n^{A_1:A_2}(t) &= -\frac{1}{2}\sum_{j=0}^{\infty} c_n(2j) T_{2j}(t) \\ &= \int_{-\pi}^{\pi} \frac{\mathrm{d}k}{2\pi} h_n(\cos\Delta_k)\Xi_{\ell_1,\ell_2,d,t}(k). \end{aligned} \tag{74}$$

Finally, this result also implies that the tripartite information identically vanishes for all times, see equation (27), in agreement with the results of [50].

5. Conclusion

In this manuscript, we provide the exact *ab initio* derivation of the formula for the dynamics of the entanglement entropies for two disjoint blocks in the spin-1/2 XY chain in a transverse magnetic field, after a global quantum quench. This result, given by equation (28), also provides a proof that the quasiparticle picture for the mutual information holds in that model, see equation (26). Our approach generalizes the one used in equation [26] for the case of a single interval. In particular, it consists in expressing the Rényi entropies of two disjoint blocks $S_n^{A_1 \cup A_2}(t)$ as a sum of terms containing the traces of even powers of the correlation matrix $\Gamma_{A_1 \cup A_2}(t)$. The evaluation of such terms amounts to that of sum of traces of different combinations of products of blocks of the correlation matrix, whose final expression is obtained via multidimensional stationary phase approximation in the scaling limit. Another direct implication of our calculation is that the tripartite information identically vanishes at all times for the XY chain, and more generally for systems where the quasiparticle picture holds.

There are some natural generalizations of our results. First, it would be interesting to see if the exact methods developed in [60, 61] can be adapted to address the quench dynamics of the negativity in the XY chain. This would prove the relation between the logarithmic negativity and the Rényi mutual information with index $n = 1/2$ after a quench [42]. Second, our calculations can probably be adapted to the case of three intervals. This would for example allow us to generalize equation (27) to study the tripartite information for disjoint intervals, and see if it also vanishes identically in that case. Finally, our results can certainly be adapted to derive exact expressions for the recently introduced entanglement asymmetry [66] and Rényi fidelities [67] in the context of disjoint intervals.

Data availability statement

The data that support the findings of this study are available upon reasonable request from the authors.

Acknowledgments

G P holds a CRM-ISM postdoctoral fellowship and acknowledges support from the Mathematical Physics Laboratory of the CRM. He also thanks SISSA for hospitality during the early stages of this project. R B acknowledges support from the Croatian Science Foundation (HrZZ) Project No. IP-2019-4-3321. We thank Pasquale Calabrese and Vincenzo Alba for useful discussions and comments on the manuscript. We also thank Rufus Boyack for sharing his proof of equation (70).

ORCID iD

Gilles Parez https://orcid.org/0000-0001-5440-9467

References

[1] Neumann J V 1929 Beweis des Ergodensatzes und des H-Theorems in der neuen Mechanik *Z. Phys.* **57** 30
[2] Greiner M, Mandel O and Bloch T H I 2002 Collapse and revival of the matter wave field of a Bose-Einstein condensate *Nature* **419** 51
[3] Kinoshita T, Wenger T and Weiss D 2006 A quantum Newton's cradle *Nature* **440** 900
[4] Cheneau M, Barmettler P, Poletti D, Endres M, Schauß P, Fukuhara T, Gross C, Bloch I, Kollath C and Kuhr S 2012 Light-cone-like spreading of correlations in a quantum many-body system *Nature* **481** 484
[5] Trotzky S, Chen Y-A, Flesch A, McCulloch I P, Schollwöck U, Eisert J and Bloch I 2012 Probing the relaxation towards equilibrium in an isolated strongly correlated one-dimensional Bose gas *Nature* **8** 325

[6] Gring M, Kuhnert M, Langen T, Kitagawa T, Rauer B, Schreitl M, Mazets I, Smith D A, Demler E and Schmiedmayer J 2012 Relaxation and Prethermalization in an isolated quantum system *Science* **337** 1318
[7] Calabrese P, Essler F H L and Mussardo G 2016 Quantum integrability in out of equilibrium systems *J. Stat. Mech.* **2016** 064001
[8] Polkovnikov A, Sengupta K, Silva A and Vengalattore M 2011 Colloquium: Nonequilibrium dynamics of closed interacting quantum systems *Rev. Mod. Phys.* **83** 863
[9] Gogolin C and Eisert J 2016 Equilibration, thermalisation and the emergence of statistical mechanics in closed quantum systems *Rep. Prog. Phys.* **79** 056001
[10] D'Alessio L, Kafri Y, Polkovnikov A and Rigol M 2016 From quantum chaos and eigenstate thermalization to statistical mechanics and thermodynamics *Adv. Phys.* **65** 239
[11] Essler F H L and Fagotti M 2016 Quench dynamics and relaxation in isolated integrable quantum spin chains *J. Stat. Mech.* **2016** 064002
[12] Cramer M, Dawson C M, Eisert J and Osborne T J 2008 Exact relaxation in a class of nonequilibrium quantum lattice systems *Phys. Rev. Lett.* **100** 030602
[13] Calabrese P 2018 Entanglement and thermodynamics in non-equilibrium isolated quantum systems *Physica* A **504** 31
[14] Deutsch J M, Li H and Sharma A 2013 Microscopic origin of thermodynamic entropy in isolated systems *Phys. Rev.* E **87** 042135
[15] Santos L F, Polkovnikov A and Rigol M 2011 Entropy of isolated quantum systems after a quench *Phys. Rev. Lett.* **107** 040601
[16] Collura M, Kormos M and Calabrese P 2014 Stationary entanglement entropies following an interaction quench in 1D Bose gas *J. Stat. Mech.* **2014** P01009
[17] Kaufman A M, Tai M E, Lukin A, Rispoli M, Schittko R, Preiss P M and Greiner M 2016 Quantum thermalization through entanglement in an isolated many-body system *Science* **353** 794
[18] Lukin A, Rispoli M, Schittko R, Tai M E, Kaufman A M, Choi S, Khemani V, Léonard J and Greiner M 2019 Probing entanglement in a many-body localized system *Science* **364** 256
[19] Brydges T, Elben A, Jurcevic P, Vermersch B, Maier C, Lanyon B P, Zoller P, Blatt R and Roos C F 2019 Probing Rényi entanglement entropy via randomized measurements *Science* **364** 260
[20] Elben A *et al* 2020 Mixed-state entanglement from local randomized measurements *Phys. Rev. Lett.* **125** 200501
[21] Neven A *et al* 2021 Symmetry-resolved entanglement detection using partial transpose moments *npj Quantum Inf.* **7** 1
[22] Vitale V, Elben A, Kueng R, Neven A, Carrasco J, Kraus B, Zoller P, Calabrese P, Vermersch B and Dalmonte M 2022 Symmetry-resolved dynamical purification in synthetic quantum matter *SciPost Phys.* **12** 106
[23] Rath A, Vitale V, Murciano S, Votto M, Dubail J, Kueng R, Branciard C, Calabrese P and Vermersch B 2022 Entanglement barrier and its symmetry resolution: theory and experiment (arXiv:2209.04393)
[24] Calabrese P and Cardy J L 2006 Time dependence of correlation functions following a quantum quench *Phys. Rev. Lett.* **96** 136801
[25] Calabrese P and Cardy J L 2007 Quantum quenches in extended systems *J. Stat. Mech.* **2007** P06008
[26] Fagotti M and Calabrese P 2008 Evolution of entanglement entropy following a quantum quench: analytic results for the XY chain in a transverse magnetic field *Phys. Rev.* A **78** 010306
[27] Alba V and Calabrese P 2017 Entanglement and thermodynamics after a quantum quench in integrable systems *Proc. Natl Acad. Sci.* **114** 7947
[28] Alba V and Calabrese P 2018 Entanglement dynamics after quantum quenches in generic integrable systems *SciPost Phys.* **4** 17
[29] Calabrese P 2020 Entanglement spreading in non-equilibrium integrable systems *SciPost Phys. Lect. Notes* 20
[30] Bennett C H, Bernstein H J, Popescu S and Schumacher B 1996 Concentrating partial entanglement by local operations *Phys. Rev.* A **53** 2046
[31] Calabrese P 2010 Entanglement entropy in conformal field theory: new results for disconnected regions *J. Stat. Mech.* **2010** P09013
[32] Fagotti M and Calabrese P 2010 Entanglement entropy of two disjoint blocks in XY chains *J. Stat. Mech.* **2010** P04016
[33] Calabrese P, Cardy J L and Tonni E 2009 Entanglement entropy of two disjoint intervals in conformal field theory *J. Stat. Mech.* **2009** P11001

[34] Alba V, Tagliacozzo L and Calabrese P 2010 Entanglement entropy of two disjoint blocks in critical Ising models *Phys. Rev.* B **81** 060411
[35] Iglói F and Peschel I 2010 On reduced density matrices for disjoint subsystems *Europhys. Lett.* **89** 40001
[36] Coser A, Tonni E and Calabrese P 2014 Entanglement negativity after a global quantum quench *J. Stat. Mech.* **2014** P12017
[37] Wolf M M, Verstraete F, Hastings M B and Cirac J I 2008 Area laws in quantum systems: mutual information and correlations *Phys. Rev. Lett.* **100** 070502
[38] Calabrese P, Cardy J L and Tonni E 2013 Entanglement negativity in extended systems: a field theoretical approach *J. Stat. Mech.* **2013** P02008
[39] Vidal G and Werner R F 2002 Computable measure of entanglement *Phys. Rev.* A **65** 032314
[40] Liu C-C, Geoffrion J and Witczak-Krempa W 2002 Entanglement negativity versus mutual information in the quantum Hall effect and beyond (arXiv:2208.12819)
[41] Alba V and Calabrese P 2019 Quantum information scrambling after a quantum quench *Phys. Rev.* B **100** 115150
[42] Alba V and Calabrese P 2019 Quantum information dynamics in multipartite integrable systems *Europhys. Lett.* **126** 60001
[43] Bertini B, Klobas K and Lu T-C 2022 Entanglement negativity and mutual information after a quantum quench: exact link from space-time duality *Phys. Rev. Lett* **129** 140503
[44] Cerf N J and Adami C 1998 Information theory of quantum entanglement and measurement *Physica* D **120** 62
[45] Hosur P, Qi X-L, Roberts D A and Yoshida B 2016 Chaos in quantum channels *J. High Energ. Phys.* JHEP02(2016)004
[46] Schnaack O, Bölter N, Paeckel S, Manmana S R, Kehrein S and Schmitt M 2019 Tripartite information, scrambling and the role of Hilbert space partitioning in quantum lattice models *Phys. Rev.* B **100** 224302
[47] Sünderhauf C, Piroli L, Qi X-L, Schuch N and Cirac J I 2019 Quantum chaos in the Brownian SYK model with large finite N: OTOCs and tripartite information *J. High Energ. Phys.* JHEP11(2019)038
[48] Kitaev A and Preskill J 2006 Topological entanglement entropy *Phys. Rev. Lett.* **96** 110404
[49] Carollo F and Alba V 2022 Entangled multiplets and unusual spreading of quantum correlations in a continuously monitored tight-binding chain (arXiv:2206.07806)
[50] Marić V and Fagotti M 2022 Universality in the tripartite information after global quenches (artXiv:2209.14253)
[51] Calabrese P and Cardy J L 2004 Entanglement entropy and quantum field theory *J. Stat. Mech.* **2004** P06002
[52] Calabrese P and Cardy J L 2005 Evolution of entanglement entropy in one-dimensional systems *J. Stat. Mech.* **2005** P04010
[53] Murciano S, Alba V and Calabrese P 2022 Quench dynamics of Rényi negativities and the quasiparticle picture *Entanglement in Spin Chains* (Berlin: Springer) p 397
[54] Parez G, Bonsignori R and Calabrese P 2021 Quasiparticle dynamics of symmetry-resolved entanglement after a quench: examples of conformal field theories and free fermions *Phys. Rev.* B **103** L041104
[55] Parez G, Bonsignori R and Calabrese P 2021 Exact quench dynamics of symmetry resolved entanglement in a free fermion chain *J. Stat. Mech.* **2021** 093102
[56] Parez G, Bonsignori R and Calabrese P 2022 Dynamics of charge-imbalance-resolved entanglement negativity after a quench in a free-fermion model *J. Stat. Mech.* **2022** 053103
[57] Alba V and Carollo F 2021 Spreading of correlations in markovian open quantum systems *Phys. Rev.* B **103** L020302
[58] Carollo F and Alba V 2022 Dissipative quasiparticle picture for quadratic markovian open quantum systems *Phys. Rev.* B **105** 144305
[59] Alba V and Carollo F 2022 Hydrodynamics of quantum entropies in ising chains with linear dissipation *J. Phys. A: Math. Theor.* **55** 074002
[60] Alba V and Carollo F 2022 Logarithmic negativity in out-of-equilibrium open free-fermion chains: an exactly solvable case (arXiv:2205.02139)
[61] Caceffo F and Alba V 2022 Entanglement negativity in a fermionic chain with dissipative defects: exact results (arXiv:2209.14164)

[62] Lieb E, Schultz T and Mattis D 1961 Two soluble models of an antiferromagnetic chain *Ann. Phys.* **16** 407
[63] Chung M C and Peschel I 2001 Density-matrix spectra of solvable fermionic systems *Phys. Rev.* B **64** 064412
[64] Peschel I 2003 Calculation of reduced density matrices from correlation functions *J. Phys. A: Math. Gen.* **36** L205
[65] Boyack R 2022 private communication
[66] Ares F, Murciano S and Calabrese P 2022 Entanglement asymmetry as a probe of symmetry breaking (arXiv:2207.14693)
[67] Parez G 2022 Symmetry-resolved Rényi fidelities and quantum phase transitions *Phys. Rev.* B **106** 235101